

Supplementary file

The Reference Phase Correction for the Fluctuated Scanning Lines and the Slope of the Stage in Tissue Characterization by Scanning Acoustic Microscope

Nguyen Thanh Phong Truong ¹, Hyehyun Kim ², Donghae Lee ¹, Yeon-Hee Kang ^{1,3}, Sungsoo Na ⁴ and Junghwan Oh ^{1,2,*}

¹ Department of Biomedical Engineering, Pukyong National University, Busan 48513, Korea; phongtruongbk@gmail.com (N.T.P.T.); ldonghae320@gmail.com (D.L.); kyhnuclear@naver.com (Y.-H.K.)

² Marine-Integrated Bionics Research Center, Pukyong National University, Busan 48513, Korea; hyehyunkim@pknu.ac.kr (H.K.)

³ (BK21 Plus) Marine-integrated Biomedical Technology Program, Pukyong National University, Busan 48513, Korea

⁴ Indiana University-Purdue University Indianapolis, Indianapolis IN 46202, USA; sungna@iu.edu (S.N.)

* Correspondence: jungoh@pknu.ac.kr (J.O.); Tel.: +82-51-629-5771; Fax: +82-51-629-5779.

Received: 10 September 2019; Accepted: 12 November 2019; Published: date

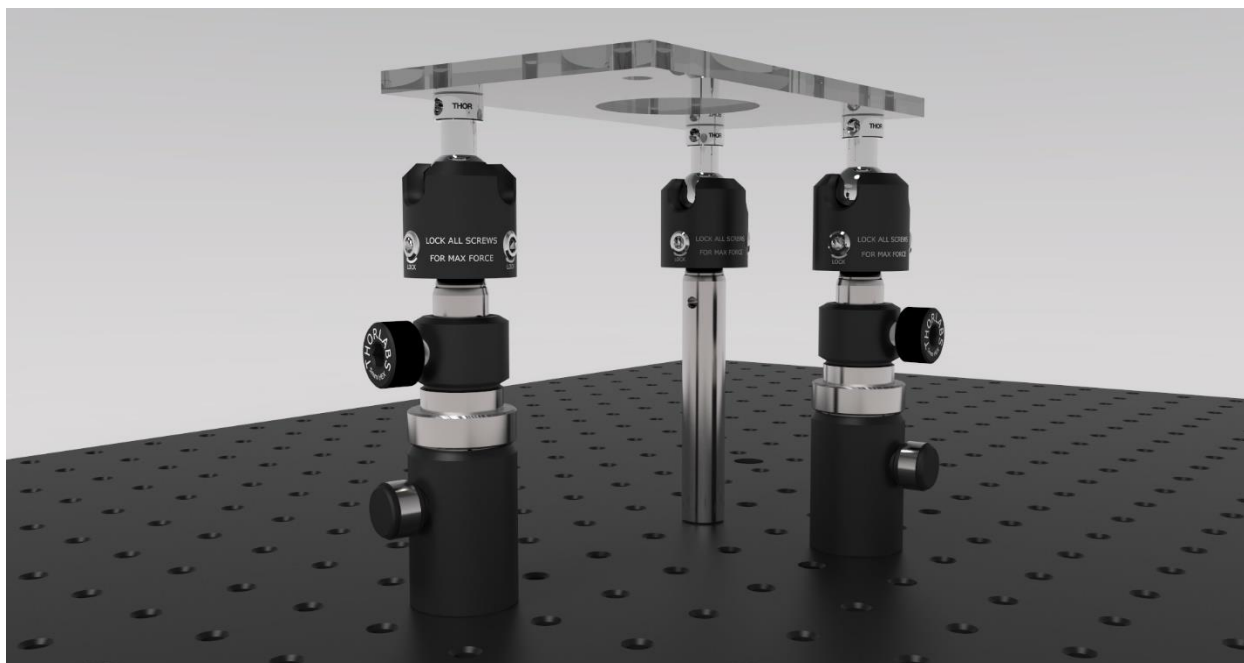


Figure S1. The slope adjustment stage. The stationary post holder, located at the origin point. The other two translatable post holders (PH2T/M, Thorlabs, New Jersey, USA), aligned along horizontal and vertical axes. The changeable height of the translatable post holders allows for changing the slope of the stage along the axes. The posts and the surface of the stage are linked by the locking ball unit (TRB1/M, Thorlabs, New Jersey, USA), due to the angle between the base and the surface of the stage created by the slope.

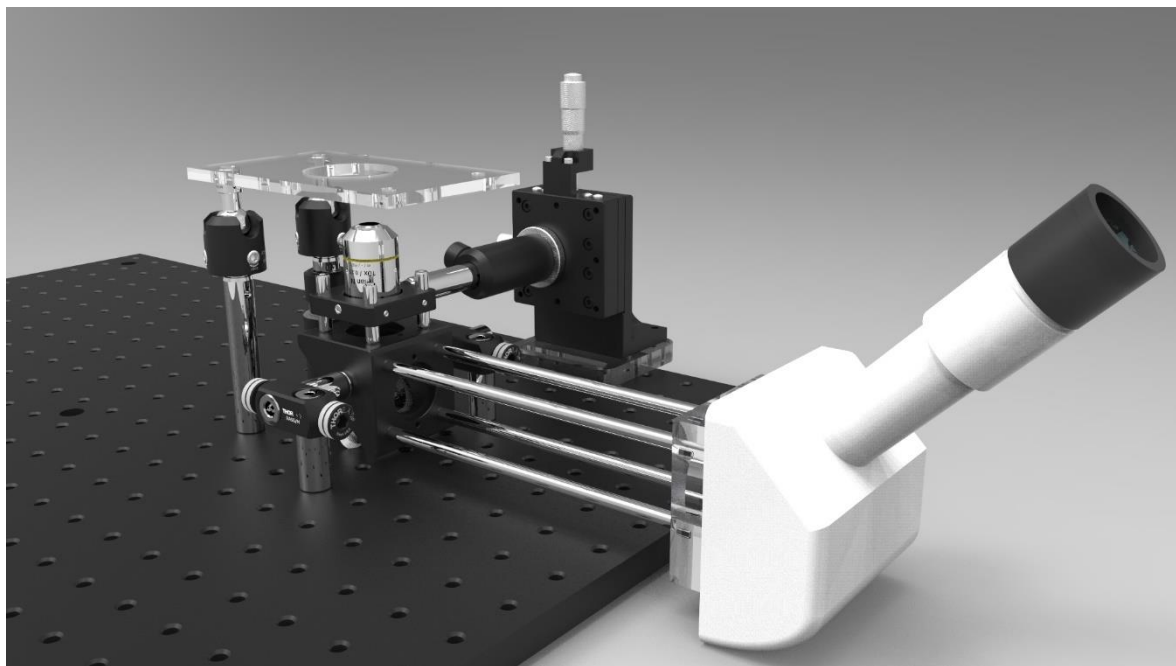


Figure S2. Integrated microscope part of the system. The part uses one objective lens to focus on the target. The objective lens holder was mounted on a vertical translator through a post holder to adjust the focus. One right-angle mirror mount (KCB1C, Thorlabs, New Jersey, USA) was used to change the direction of the light head to eye piece.

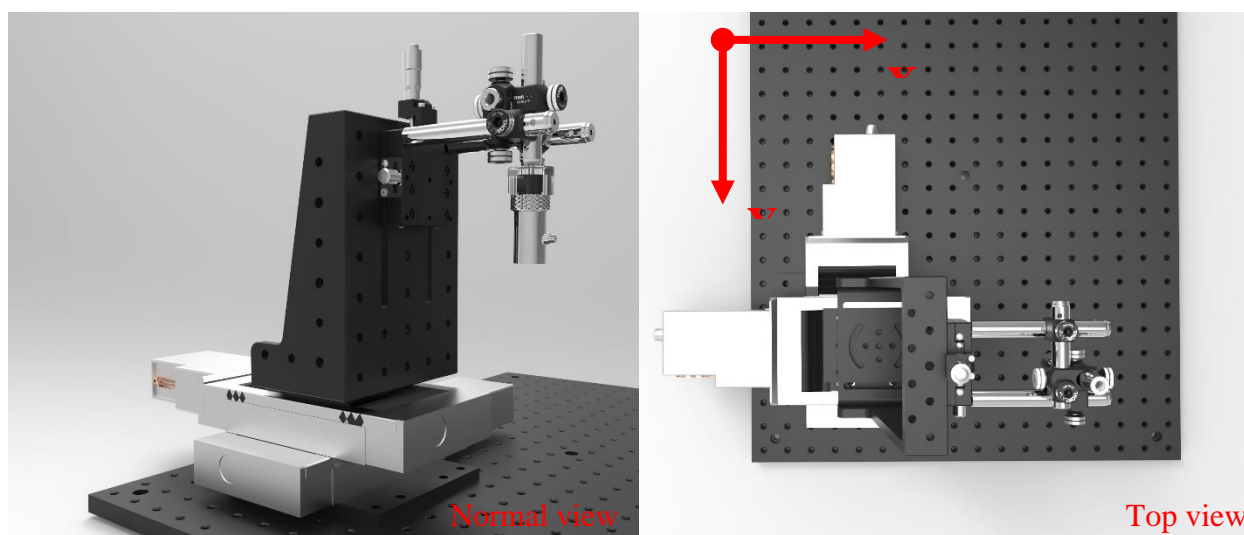


Figure S3. A pair of linear scanning motors. The top motor is the scanning motor. The bottom motor is the advance motor. The scanning motor is defined as X axis. The advance motor is defined as Y axis.

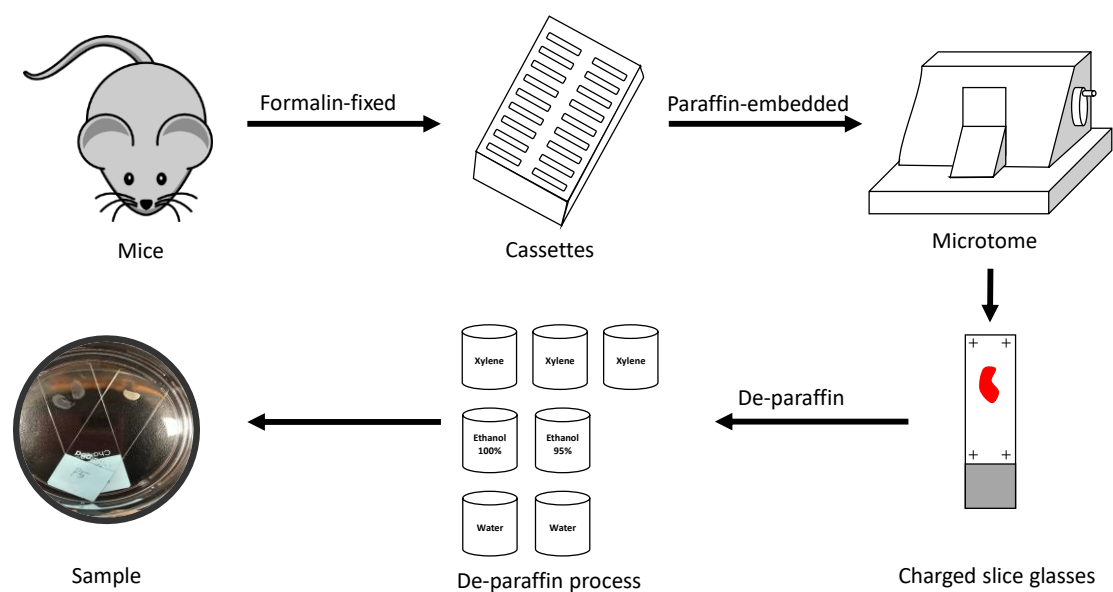


Figure S4. Schematic illustration of tissue processing. Tumor was collected, fixed in 10% neutral buffered formalin, dehydrated, embedded with paraffin, sectioned in 20 μm thick, and attached on charged slice glasses. Before scanning, the sample went through the de-paraffin process to remove paraffin.

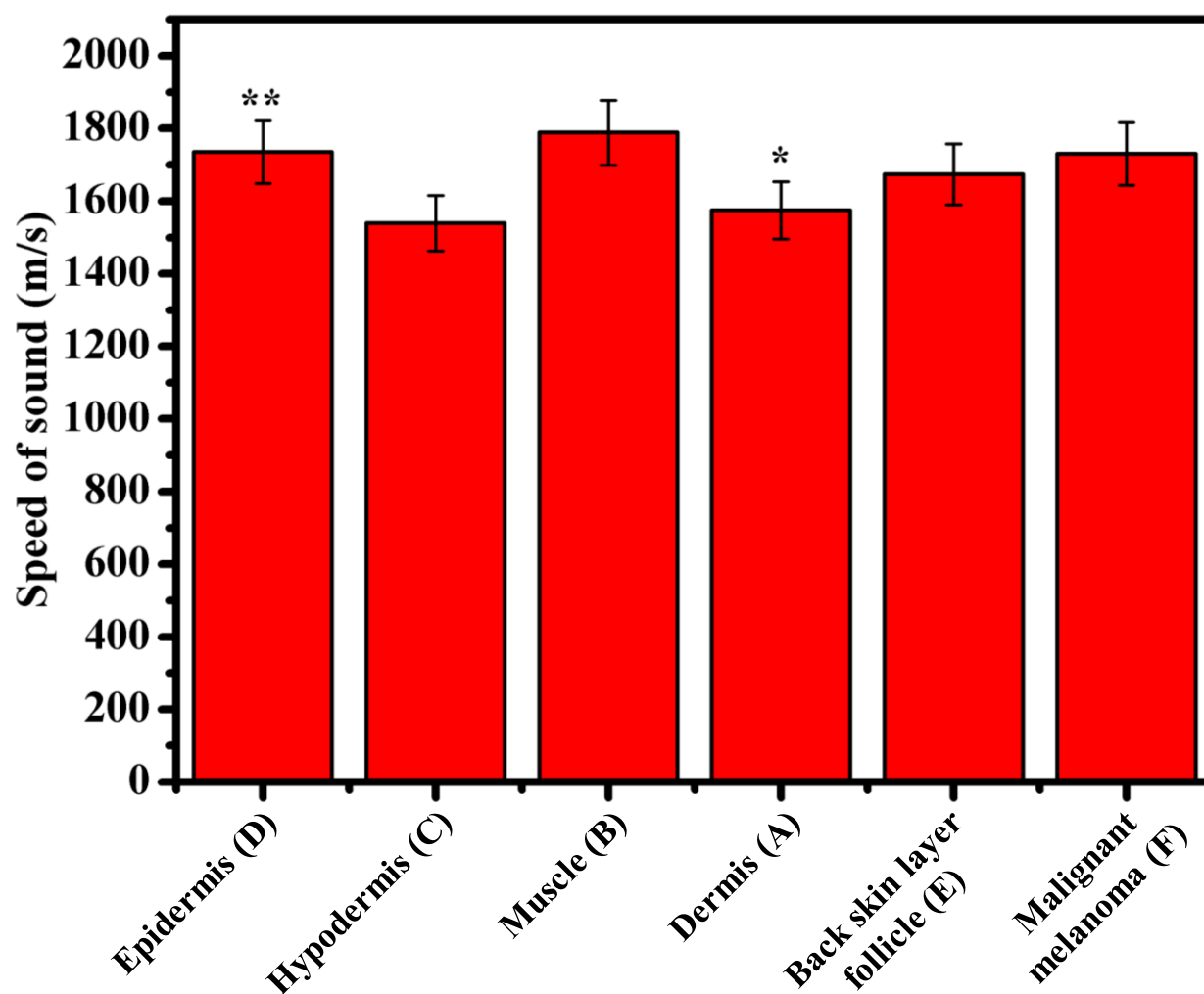


Figure S5. Average speed of sound. Data were expressed as mean \pm S.D. ($n = 3$, * $p < 0.05$, ** $p < 0.01$).

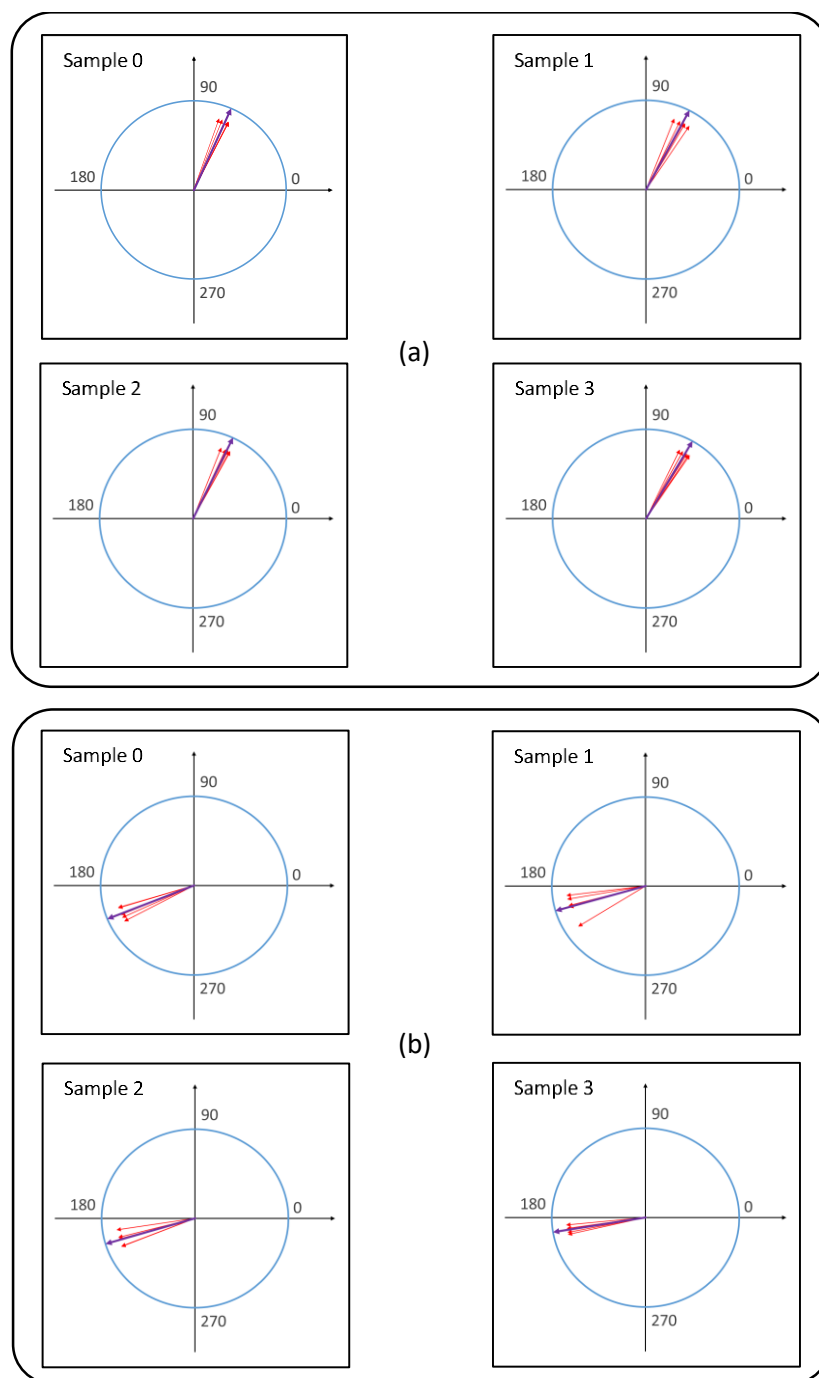


Figure S6. Graphs of the phase values from Table S1. The phase values at 33 MHz (a) and 80 MHz (b), respectively. The red arrows show the value of individual phases, while the purple arrows indicate its average value.

Table S1. The typical values of phase (in degree units) caused by random noise.

Sample number	Sample 0		Sample 1		Sample 2		Sample 3	
	33 MHz	80 MHz	33 MHz	80 MHz	33 MHz	80 MHz	33 MHz	80 MHz
1	68.576	208.128	64.501	195.106	65.624	201.742	56.683	188.992
2	63.555	197.326	61.6	196.372	69.051	195.888	64.895	188.204
3	63.823	196.984	60.391	187.102	62.12	188.856	57.657	192.901
4	64.269	202.667	69.126	212.449	63.744	201.809	58.971	185.671
5	71.265	204.953	56.782	190.03	62.513	194.567	62.51	191.53
Average	66.2976	202.0116	62.48	196.2118	64.6104	196.5724	60.1432	189.4596
SD	±3.450612	±4.840541	±4.633014	±9.824691	±2.832761	±5.435522	±3.453606	±2.840707